LANGMUIR

Interfaces: Adsorption, Reactions, Films, Forces, Measurement Techniques, Charge Transfer, Electrochemistry, Electrocatalysis, Energy Production and Storage

Thermogravimetric Analysis and Mass Spectrometry Allow for Determination of Chemisorbed Reaction Products on Metal Organic Frameworks

William Matthew Jones, Jesus B Tapia, Robert R Tuttle, and Melissa M. Reynolds

Langmuir, **Just Accepted Manuscript** • DOI: 10.1021/acs.langmuir.0c00158 • Publication Date (Web): 03 Mar 2020

Thermogravimetric Analysis and Mass Spectrometry Allow for Determination of Chemisorbed Reaction Products on Metal Organic Frameworks

W. Matthew Jones[†], Jesus B. Tapia[†], Robert R. Tuttle[†], and Melissa M. Reynolds*[†‡§]

[†]Department of Chemistry, [‡]School of Biomedical Engineering, and [§]Chemical and Biological Engineering, Colorado State University, Fort Collins, Colorado 80523, United States

Abstract

Thermogravimetric analysis (TGA) is a technique which can probe chemisorption of substrates onto metal organic frameworks. A TGA method was developed to examine the catalytic oxidation of *S*-nitrosoglutathione (GSNO) by the MOF $H_3[(Cu_4Cl)_3(BTTri)_8]$ (abbr. Cu-BTTri; H_3BTTri = 1,3,5-tris(1*H*-1,2,3-triazol-5-yl)benzene), yielding glutathione disulfide (GSSG) and nitric oxide (NO). Thermal analysis of reduced glutathione (GSH), GSSG, GSNO, and Cu-BTTri revealed thermal resolution of all four analytes through different thermal onset temperatures and weight percent changes. Two reaction systems were probed: an aerobic column flow reaction and an anaerobic solution batch reaction with gas agitation. In both systems, Cu-BTTri was reacted with a 1 mM GSH, GSSG, or GSNO solution, copiously rinsed with distilled-deionized water (dd-H_2O), dried (25 °C, <1 Torr), and assessed by TGA. Additionally, stock, effluent or supernatant, and rinse solutions for each glutathione derivative within each reaction system were assessed by mass spectrometry (MS) to inform on chemical transformations promoted by Cu-BTTri as well as relative analyte concentrations. Both reaction systems exhibited chemisorption of glutathione derivatives to the MOF by TGA. Mass spectrometry analyses revealed that in both systems, GSH was oxidized to GSSG, which chemisorbed to the MOF whereas GSSG remained unchanged during chemisorption. For GSNO, chemisorption to the MOF without reaction was observed in the aerobic column setup, whereas conversion to GSSG and subsequent chemisorption was observed in the anaerobic batch setup. These findings suggest that, within this reaction system, GSSG is the primary adsorbent of concern with regards to strong binding to Cu-BTTri. Development of similar thermal methods could allow for the probing of MOF reactivity for a wide range of systems, informing on important considerations such as reduced catalytic efficiency from poisoning, recyclability, and loading capacities of contaminants or toxins with MOFs.

Introduction

Metal organic frameworks (MOFs), due to their chemical versatility, extensive porosity, and structural tunability, are attractive substrates for applications in catalysis and photocatalysis, aqueous remediation, chemical separations, gas capture and storage, electrochemistry, and biomedicine.[1-14] The relative efficacy and performance of MOFs in many of these applications is

dependent on adsorption and desorption phenomena of guest or solvent species to the frameworks and subsequent chemical interactions or reactions. Consequently, irreversible chemisorption of analytes, interferents, or reaction starting materials, products, and by-products is a concern for the sustained use, reuse, and recyclability of MOFs for many applications.[15] This issue is especially significant in catalysis and chemical sensing applications due to potential diminished efficacy of the MOF and the inability to use traditional regeneration methods, such as heating at elevated temperatures, to decompose or desorb the bound analytes.[3, 7, 13-14, 16] The development of analytical techniques to probe chemisorption of reaction starting materials and products to MOFs is thus an important consideration for improved understanding of how MOFs are most effectively used in the aforementioned applications.

Thermogravimetric analysis (TGA) is a widely used technique for measuring thermal phenomena of analytes. Samples analyzed by TGA are subjected to a programmed heating cycle in a closed system with a defined atmosphere while the mass change of a sample is monitored with respect to temperature or time. Mass changes observed can be correlated to various thermochemical processes, notably thermal decomposition, dehydration, or desorption of guest or solvent species of the analyte.[17] The abstracts of current MOF literature indicate the routine use of TGA for discerning the thermal stability of the as-synthesized MOFs. Additionally, some TGA studies on MOFs focus on the thermal stability of a framework with an impregnated, intercalated, or chemisorbed analyte as compared to the thermal stability of the neat MOF.[15, 18-28] However, in terms of chemisorbed analytes, there is limited mention of TGA being used as a screening technique to elucidate information about reaction systems, such as determining if reaction products or by-products undergo irreversible chemisorption to MOFs in catalysis.

The reaction system of interest for this work focuses on the copper-based MOF $H_3[(Cu_4Cl)_3(BTTri)_8]$ (abbr. Cu-BTTri; H_3BTTri = 1,3,5-tris(1*H*-1,2,3-triazol-5-yl)benzene)[29] and its interactions with *S*-nitrosoglutathione (GSNO) as well as reduced glutathione (GSH) and glutathione disulfide (GSSG). Research has shown Cu-BTTri catalyzes the oxidation of GSNO to yield nitric oxide (NO) and GSSG.[30] The NO release from GSNO has important implications for implanted biomedical devices due to the ability of NO to promote vasodilation, antithrombotic activity, and biofilm reduction.[30-32] Despite investigation of the mechanism and reaction stoichiometry for NO release from GSNO catalyzed by Cu-BTTri, the ability of glutathione derivatives (abbr. GS-X) to irreversibly bind to the MOF has yet to be determined.[30] Binding of these substrates could lead to deactivation of the MOF catalytic activity, preventing sustained nitric oxide release from a biomedical device for the desired therapeutic effects. Furthermore, the chemical similarity between the three GS-X analytes invokes the question as to whether their subtle differences in structure could be distinguished using TGA and mass spectrometry (MS)

methods, allowing for discernment between the substrates if all three analytes were capable of binding to the MOF.

Herein, we report a TGA method for identifying chemisorbed structurally similar substrates in a MOF catalysis system. Assessment of anaerobic batch reactions with Cu-BTTri powder and GS-X solutions with agitation by bubbling was performed to limit loading of the analytes into the pores of the MOF by processes other than diffusion. Additionally, assessment of aerobic column reactions between Cu-BTTri powder and GS-X solutions was performed to maximize forced loading of the analytes into the pores of the MOF. Comparison of the thermal decomposition profiles of the Cu-BTTri batch reaction samples and the Cu-BTTri column reaction samples to the thermal decomposition profiles of Cu-BTTri alone lead to elucidation of which substrates strongly bind to the MOF during batch or flow catalysis. Furthermore, mass spectrometry is used as a complimentary technique to assess the composition of the substrate solutions before, during, and after the reactions to corroborate the TGA data. Comparison of the mass spectra for the stock solutions, reaction effluent or supernatant solutions, and the rinse solutions for each GS-X solution can inform on chemical transformations performed by the MOF, the procedure for rinsing adventitious analyte from the framework pores, and the identity of the bound analytes associated with the given thermal decomposition profiles. These studies show that TGA can be used as a rapid, informative technique for assessing chemisorption of reaction components to MOFs, leading to perspectives on protocols for continued use or reuse/recycling of MOFs for catalysis or chemical sensing applications.

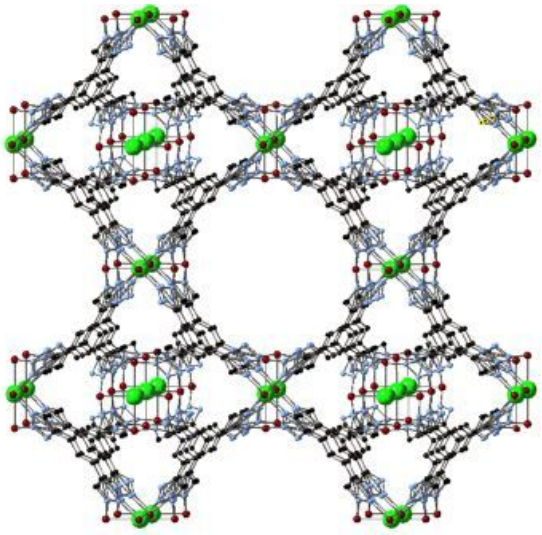

Figure 1. Structure of MOF Cu-BTTri, $H_3[(Cu_4Cl)_3(BTTri)_8]$. Carbon atoms depicted in black; chlorine atoms depicted in green; copper atoms depicted in red; hydrogen atoms omitted for clarity; nitrogen atoms depicted in blue.

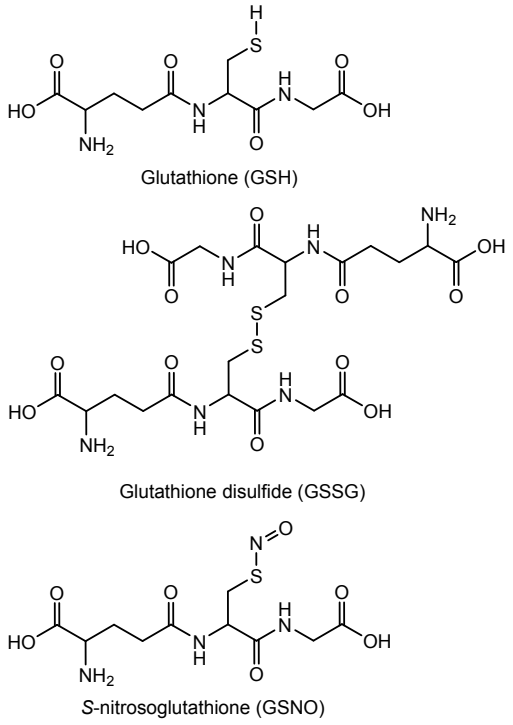

Figure 2. Structures of glutathione (GSH), glutathione disulfide (GSSG) and *S*-nitrosoglutathione (GSNO).

Experimental

Chemicals and Reagents: The following chemicals and reagents were used as received: acetone (99.5%, Sigma-Aldrich), bis(triphenylphosphine)palladium(II) dichloride (99.99%, Sigma-Aldrich), chloroform-*d* (99.8% D, Cambridge Isotopes Laboratories) copper(II) chloride (99%, EMD), copper(I) iodide (98%, Alfa Aesar), deuterium oxide (99.9% D, Cambridge Isotopes Laboratories), dichloromethane (99.8%, Sigma-Aldrich), diethyl ether (99%, Fisher), N,N-dimethylformamide (99.9%, Fisher; abbr. DMF), dimethylsulfoxide-*d*6 (99.9% D, Cambridge Isotopes Laboratories), dinitrogen (ultra-high purity, Airgas), L-glutathione, oxidized (98%, Sigma-Aldrich; abbr. GSSG), glutathione, reduced (98%, AMRESCO; abbr. GSH), hydrochloric acid (35.0–38.0%, Fisher), methanol (99.9%, Fisher; 99.9%, HPLC, EMD Millipore), silica gel (0.060–0.2 mm, 70-230 mesh, Alfa Aesar), sodium hydroxide (98.9%, Fisher), sodium nitrite (97.0%, EMD; 99.999%, Alfa-Aesar), trimethylsilylacetylene (99%, Chem-Impex International), 1,3,5-tribromobenzene (98%, Alfa Aesar), and trimethylsilyl azide (94%, Alfa Aesar). Distilled-deionized water (abbr. dd-H_2O) with a minimum resistance of 18.2 MΩ·cm was prepared using a Millipore Direct-Q 5 water purification system (EMD Millipore). Diethylamine (99%, Alfa Aesar) was freshly distilled under a dinitrogen atmosphere prior to use.

Synthetic Methods: ***S*-Nitrosoglutathione**: In a typical reaction, *S*-nitrosoglutathione (abbr. GSNO) was prepared following an adapted protocol of the method reported by Hart.[33] Reduced glutathione (1.54 g, 5.0 mmol) was suspended in dd-H_2O (8 mL) and dissolved with the addition of 2 M hydrochloric acid (2.5 mL). The reaction was cooled to 0 °C using an ice-water bath, and sodium nitrite (0.345 g, 5.0 mmol) was added. The reaction was immediately shielded from light and stirred for 40 minutes at 0 °C. The resulting mixture was filtered to isolate a reddish-pink precipitate, which was subsequently washed with 5 × 5 mL of 0–5 °C dd-H_2O and 3 × 5 mL of acetone. The product was placed under dynamic vacuum (<100 mTorr) for 4 h to remove residual solvent, affording 0.865 g of GSNO (51% yield; 98.6% pure, UV-Vis analysis). The obtained product was stored light-free in a −20 °C freezer when not in use. ^{1}H NMR (400 MHz, D_2O): 4.70-4.61 (m, 1H), 4.20-3.90 (m, 2H), 3.93 (s, 2H), 3.78 (t, 1H, J = 6.4 Hz), 2.42 (t, 2H, J = 7.6 Hz), 2.18-2.01 (m, 2H).[34] UV-vis (H_2O): 335 ($\pi \rightarrow \pi^*$), 545 ($n_N \rightarrow \pi^*$).[33]

H_3BTTri: In a typical reaction, 1,3,5-tris(1*H*-1,2,3-triazol-5-yl)benzene (H_3BTTri) was prepared following the literature protocols given by Demessence et al.[29] Solid 1,3,5-tribromobenzene (9.45 g, 30.0 mmol) was dissolved in diethylamine (250 mL) with stirring under an inert atmosphere (N_2). Copper(I) iodide (50 mg, 0.26 mmol) and bis(triphenylphosphine)palladium(II) dichloride (400 mg, 0.57 mmol) were added to the solution. Trimethylsilylacetylene (10.6 g, 108. mmol) was added to the solution, and the resulting mixture was stirred at 50 °C for 6 h. Formed diethylamine hydrobromide was removed by filtration and washed with ether (45 mL). Combined washings were evaporated to dryness under dynamic vacuum (<100 mTorr), and the resulting product was purified by a silica plug to yield 9.61 g (78%) 1,3,5-tris(trimethylsilylethynyl)benzene as an intermediate. ^{1}H NMR (400 MHz, $CDCl_3$): δ = 7.43 (s), 0.23 (s) ppm.

The 1,3,5-tris(trimethylsilylethynyl)benzene intermediate (9.61 g, 26.3 mmol) was hydrolyzed by treatment with aqueous sodium hydroxide (30 mL, 1 M), dichloromethane (20 mL), and methanol (50 mL) with stirring at 25 °C for 3 h. Evaporation of methanol, ether extraction of the residue, and evaporation of the solvent under dynamic vacuum (<100 mTorr) yielded 2.68 g of white powder containing 1,3,5- triethynylbenzene. ^{1}H NMR (400 MHz, $CDCl_3$): δ = 7.51 (s), 3.12 (s) ppm.

Trimethylsilylazide (9.26 g, 80.4 mmol) was added to a mixture of copper(I) iodide (510 mg, 2.63 mmol) and 1,3,5-triethynylbenzene (2.68 g, 17.8 mmol) in dimethylformamide (90 mL) and methanol (10 mL) under an inert atmosphere (N_2). The resulting mixture was stirred at 100 °C for 36 h. The mixture was filtered and reduced to a volume of 10 mL via rotary evaporation. A pale-yellow precipitate was formed upon the addition of dd-H_2O (30 mL) to the resulting filtrate. The solid was collected by filtration, washed with ether, and dried under dynamic vacuum (<100

mTorr) to yield 4.1 g (83%) of the product. ^{1}H NMR (400 MHz, $(CD_3)_2SO$): δ = 8.52 (s), 8.34 (s) ppm.

$H_3[(Cu_4Cl)_3(BTTri)_8]$: In a typical reaction, $H_3[(Cu_4Cl)_3(BTTri)_8]$ (Cu-BTTri) was prepared following the literature protocols given by Demessence et al.[29] A solution of H_3BTTri (225 mg, 0.937 mmol) in dimethylformamide (40 mL) was prepared in a 250 mL Pyrex bottle. Solid $CuCl_2{\cdot}2H_2O$ (383 mg, 2.25 mmol) was added to the solution. The mixture was heated at 100 °C for 72 h to afford $H_3[(Cu_4Cl)_3(BTTri)_8(DMF)_{12}]{\cdot}7DMF{\cdot}76H_2O$. The mixture was filtered, and the resulting purple powder was washed with boiling DMF (10 x 10 mL) and allowed to dry under ambient conditions to yield 218 mg (76%) of product. Solvent exchange was performed with dd-H_2O via soxhlet extraction for 48 h to ensure ligand and solvent exchange of DMF to H_2O and to remove any residual copper ions. The MOF was analyzed by powder X-ray diffraction (pXRD) and found to match a literature standard (SI-Figure 1).[29] The MOF was used for experimentation in the hydrated form with a theoretical formula of $H_3[(Cu_4Cl)_3(BTTri)_8{\text{-}}(H_2O)_{12}]{\cdot}72H_2O$.

Reaction Systems: **Aerobic Cu-BTTri Column Reactions**: Four 1 mL empty fritted, solid phase extraction (SPE) tubes were packed with Cu-BTTri (30 mg, 7.0 μmol) under ambient conditions. For the first column, dd-H_2O (20 mL) was passed through the MOF bed using pressurized air. The MOF was removed from the column and vacuum dried overnight (<1 Torr) for TGA as a control for behavior of hydrated Cu-BTTri. For the remaining three columns, freshly prepared aqueous solutions of GSH, GSSG, and GSNO (20 mL, 1 mM) were separately passed through the MOF beds using pressurized air. The columns were subsequently rinsed with dd-H_2O (100 mL; 10 x 10 mL) using pressurized air and vacuum dried overnight (<1 Torr), and MOF samples were removed from the columns for TGA. For each column reaction, a 1 mL aliquot of the 1mM stock solution, 20 mL column effluent, and each 10 mL rinse solution (10 total) was passed through 2 consecutive 0.2 μm syringe filters and subsequently assessed by mass spectrometry. **Anaerobic Cu-BTTri Bubbling Reactions**: Three 50 mL, 3-neck round bottom flasks were loaded with Cu-BTTri (50 mg, 11.6 μmol), dried overnight at 110 °C, evacuated using dynamic vacuum (<100 mTorr) for 1 h, and placed under a dinitrogen atmosphere at 25 °C. Fresh aqueous solutions of GSH, GSSG, and GSNO (1 mM, ~ 35 mL, 35 μmol) were prepared anaerobically and shielded from light. These solutions were separately cannula transferred to one of the three reaction flasks under a dinitrogen atmosphere at 25 °C. The mixtures were immediately shielded from light with aluminum foil and agitated using a dinitrogen purge for 72 h at 25 °C. Aliquots (1 mL) of the reaction supernatants were isolated both anaerobically and aerobically, passed through 2 consecutive 0.2 μm syringe filters, and subsequently assessed by mass spectrometry. Wet MOF particles were aerobically transferred to three separate 1 mL empty fritted, SPE tubes for rinsing. The MOF particles were subsequently rinsed with dd-H_2O (100 mL; 10 x 10 mL) using pressurized air and vacuum dried overnight (<1 Torr), and MOF samples were

removed from the columns for TGA. A 1 mL aliquot of each 10 mL rinse solution (10 total) was passed through 2 consecutive 0.2 μm syringe filters and subsequently assessed by mass spectrometry.

Physical Methods and Instrumentation: **Sample handling**: Experimental techniques and sample handling were performed on the benchtop or on a dual-manifold Schlenk line (<100 mTorr) using dinitrogen in the inert gas manifold. **NMR analyses**: Proton nuclear magnetic resonance (^{1}H NMR) spectroscopy was performed using a Bruker AVANCE NEO 400 spectrometer to observe ^{1}H nuclei. Samples were dissolved in deuterium oxide (D_2O), and spectra were acquired at 400 MHz from 32 transients at 25 °C. Chemical shifts were referenced to the solvent peak (HDO; 4.790 ppm). **UV-Vis analyses**: Ultraviolet-visible (UV-vis) spectra were obtained in 1.0 cm quartz cuvettes using a Nicolet Evolution 300 spectrophotometer. **pXRD analysis**: Powder X-ray diffraction (pXRD) analyses were performed using a Bruker D-8 Discover DaVinci X-ray diffractometer using a Cu-Kα source. *MS analyses:* Mass spectra were obtained using an Agilent 6224 time-of-flight mass spectrometer (TOF-MS) equipped with a dual electrospray ionization source operated in positive ion mode using HPLC methanol as the mobile phase. **Thermal analyses**: Thermogravimetric analyses (TGA) were performed using a TA Instruments TGA Q500 instrument equipped with a standard ceramic furnace. Ultra-high purity (UHP) dinitrogen was used as the purge gas at a flow rate of 40 mL·min^{-1} for the balance purge and 60 mL·min^{-1} for the furnace purge. Samples (~ 1-10 mg) were contained in alumina ceramic crucibles resting in platinum sample pans. Thermal methods were programmed as follows: ramp 5 °C min^{-1}, isothermal @ 25 °C for 30 min; ramp 5 °C min^{-1} to 100 °C; isothermal @ 100 °C for 10 min; ramp 5 °C min^{-1} to 225 °C; isothermal @ 225 °C for 10 min.

Data reporting and statistical analysis: All data were reported as a mean ± standard deviation of n ≥ 3 replicate measurements. Statistical difference was determined using two-tailed Student's t-test ($p = 0.05$) or Analysis of variance (ANOVA, $p = 0.05$). Thermal decomposition temperatures were determined using the Onset Point analysis function with the TRIOS (v. 4.2.1.36612, TA Instruments) software platform. Due to the 100 °C and 225 °C isotherms used for the thermal method, thermal phenomena and associated weight changes were calculated using 101 °C and 220 °C for the defined temperature ranges.

Results and Discussion

I. Thermal Transitions for Glutathione Derivatives and Cu-BTTri

Discerning whether GS-X species have adsorbed to the MOF Cu-BTTri with thermal methods depends on some key questions. 1) Do GSH, GSSG, and GSNO exhibit different, resolvable thermal decomposition phenomena allowing for their identification? 2) Does Cu-BTTri alone exhibit any thermal decomposition or desolvation phenomena that overlap or inhibit the resolution

of GS-X thermal phenomena? 3) Does Cu-BTTri with bound GS-X analytes exhibit distinguishable thermal phenomena from the analytes or MOF alone? 4) Can a secondary method (such as mass spectrometry) be employed to corroborate the adsorption and identification of GS-X species to the MOF? Answers to these questions are important for conclusively demonstrating chemisorption to the MOF without the use of direct chemical identification methods.

Thermal decomposition of GSH, GSSG, and GSNO was assessed to confirm that all three compounds were resolvable via TGA. The determined thermal decomposition temperatures are reported in Table 1 with representative thermograms for each analyte shown in Figure 3. For GSH, no change in mass is observed until thermal decomposition occurs at 192 (± 1) °C, which is consistent with literature values.[34-35] Therefore, GSH does not lose adventitious water prior to its decomposition. For GSSG, 6.4 (± 0.8) % mass loss is observed up until the 100 °C isotherm, indicating that GSSG undergoes dehydration and is susceptible to adsorption of adventitious water from ambient air. Thermal decomposition of GSSG occurs at 179 (± 1) °C, consistent with the reported melting point of GSSG.[35] For GSNO, less than 1 % mass loss is observed up until the 100 °C isotherm, indicating GSNO may contain a very small amount of adventitious water. Two thermal decomposition transitions are observed for GSNO. The first transition, observed at 143 (± 1) °C, is attributed to homolytic cleavage of the S-N bond resulting in evolution of NO. The decomposition temperature is shifted from the literature reported value for the thermal cleavage of the S-N bond by ~ 8 °C,[36] but this shift can be attributed to differences in experimental design and thermal heating parameters. The second transition, observed at 189 (± 1) °C, is attributed to thermal decomposition of the remaining residue after loss of NO. Previous research has shown that thermal decomposition of GSNO results in formation of NO and GSSG following the equation $2\,\mathrm{GSNO} \rightarrow 2\,\mathrm{NO} + \mathrm{GSSG}$, which is consistent with the observed secondary thermal decomposition event.[36] The thermal decomposition transitions for all three analytes are significantly different ($p < 0.001$), confirming the resolution of all three glutathione derivatives by the TGA programming selected. This finding suggests that the analytes can possibly be resolved when chemisorbed to the MOF Cu-BTTri.

Table 1. Thermal Transitions of Glutathione Derivatives Measured by TGA

Substrate	Onset Temperature (T_o - °C)[a,b,c]	
GSH	192 (± 1)	-
GSSG	179 (± 1)	-
GSNO	143 (± 1)	189 (± 1)

[a] T_o calculated using TRIOS software; ΔT of 101-220 °C for GSH/GSSG; ΔT_1 of 101-155 °C, ΔT_2 of 155 – 220 °C for GSNO.
[b] Data reported as mean ± SD of $n = 3$ replicate measurements.

[c] Ramp 5 °C min^{-1} to 25 °C; isothermal @ 25 °C for 30 min; ramp 5 °C min^{-1} to 100 °C; isothermal @ 100 °C for 10 min; ramp 5 °C min^{-1} to 225 °C; isothermal @ 225 °C for 10 min.

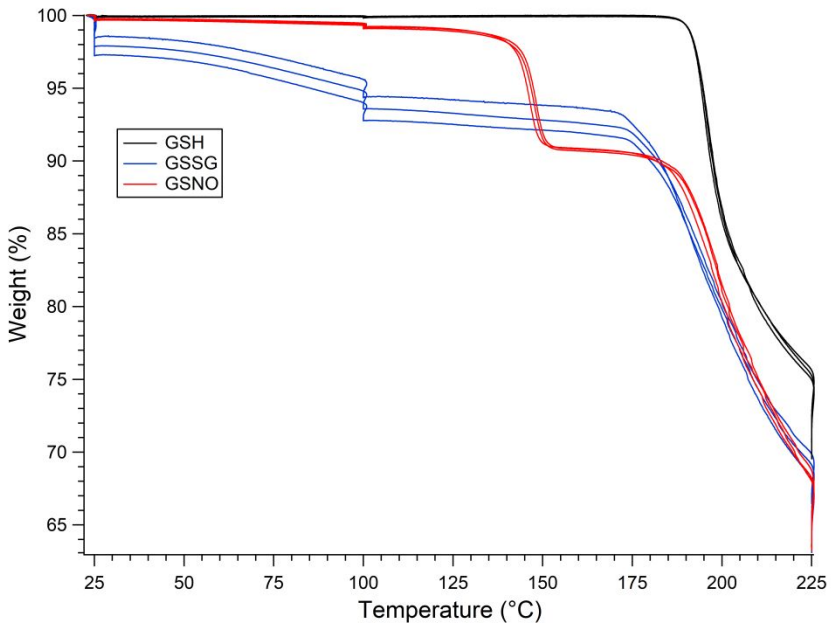

Figure 3. Resolution of the thermal decomposition phenomena of GSH (black), GSSG (blue), and GSNO (red) by TGA. Replicate measurements (n = 3) are shown for each sample.

For the MOF Cu-BTTri, Demmessence et. al. used TGA to determine that hydrated Cu-BTTri contains up to 33 wt. % H_2O under ambient conditions, and these waters of hydration are easily removed with gentle heating.[29] Furthermore, p-XRD studies indicated that Cu-BTTri retains crystallinity until at least 270 °C.[29] Hydrated Cu-BTTri was assessed by TGA after drying overnight at 25 °C (< 1 Torr), and the results of this work are consistent with the literature. As shown in Table 2 and Figure SI-7, the MOF exhibits extensive dehydration of adsorbed water at 25 °C, and dehydration is essentially complete at 100 °C, with an average mass loss of 12 (± 8) wt. % observed up to 101 °C. The large variability in this change in wt. % is attributed to the TGA auto-sampling methodology as dried Cu-BTTri can adsorb H_2O from ambient conditions while sitting in the TGA sample pans. Between 101 and 220 °C only 1.1 (± 0.1) wt. % change is observed, indicating that Cu-BTTri does not display thermal phenomena over this temperature range aside from continued, albeit minimal, dehydration. Table 3 gives the onset point for this continued dehydration phenomenon as 144 (± 3) °C. The lack of thermal transitions from 101 – 220 °C for dried Cu-BTTri allow any thermal phenomena observed over this temperature range to be directly attributed to the presence of an adsorbed glutathione derivative and not the MOF.

Table 2. Weight Change of Cu-BTTri from Ambient Conditions by TGA

Cu-BTTri Weight Change from Ambient Conditions[a,b,c]	
ΔT	Δ wt. %
25 – 101 °C	12 (± 8)
101 – 220 °C	1.1 (± 0.1)

[a] Data reported as mean ± SD of n = 3 replicate measurements.
[b] Ramp 5 °C min^{-1} to 25 °C; isothermal @ 25 °C for 30 min; ramp 5 °C min^{-1} to 100 °C; isothermal @ 100 °C for 10 min; ramp 5 °C min^{-1} to 225 °C; isothermal @ 225 °C for 10 min.
[c] 30 mg MOF Cu-BTTri loaded into 1 mL empty fritted SPE tube; 20 mL of dd-H_2O flowed through MOF bed; vacuum dried (~ 1 Torr)

II. Thermal Transitions and Associated Mass Spectra for Aerobic Cu-BTTri Column Reactions with Glutathione Derivatives

Column reaction systems were prepared to model whether GSH, GSSG, and GSNO would strongly bind to Cu-BTTri in aqueous reaction media and produce distinct thermal decomposition profiles by TGA, allowing for discernment of bound glutathione derivatives from reactions with Cu-BTTri. The procedure for studying this reaction system is given below in Scheme 1. By passing GS-X (where X = H, SG, NO) solutions over the MOF and subsequently rinsing with H_2O, any remaining species would be strongly bound to the MOF as opposed to being adventitiously trapped in the pores of the framework. Bound species should give distinct thermal decomposition profiles compared to the observed dehydration phenomenon of Cu-BTTri alone. Additionally, mass spectrometry was employed to compare the GS-X stock solutions, the effluent solutions passed through the MOF column, and the column rinse solutions. Tracking the effluent and rinsing solutions assesses what changes, if any, the analytes undergo during or after exposure to the MOF. Furthermore, detection of analytes in the rinse solutions is important for ensuring the MOF has been sufficiently rinsed and indicates what analytes are strongly bound to the framework, giving rise to any new thermal decomposition profiles observed.

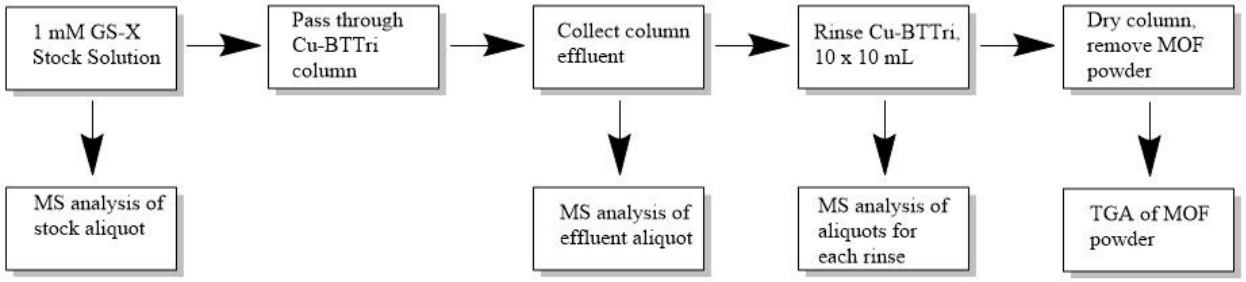

Scheme 1. Flowchart for the procedure and analysis of the aerobic Cu-BTTri column reactions with glutathione derivatives.

Table 3 gives the thermal onset temperatures and associated wt. % changes for Cu-BTTri samples exposed to dd-H_2O, 1 mM GSH, 1 mM GSSG, and 1 mM GSNO. For Cu-BTTri exposed to 1 mM GSH and 1 mM GSSG, both systems are significantly different from the hydrated Cu-BTTri control in both T_o ($p < 0.001$) and wt. % Δ ($p = 0.00056$), indicating adsorption of GS-X species to the MOF. Despite differences in the thermal decomposition temperatures of GSH and GSSG, these two analytes do not exhibit statistical difference ($p = 0.098$) in their thermal decomposition temperatures when adsorbed to Cu-BTTri. For Cu-BTTri exposed to 1 mM GSNO, a T_o of 167 (± 1) °C was found to be significantly different ($p = 0.00052$) from both MOF exposure to GSH and GSSG as well as the hydration control. This result is unsurprising given the marked differences in the thermal decomposition of GSNO compared to GSH and GSSG. However, the weight change of 2.1 (± 0.1) wt. % Δ for the GSNO exposure was consistent with the weight changes for GSH and GSSG exposures ($p = 0.26$), indicating a similar amount of chemisorption of all three analytes to the MOF.

Table 3. Thermal Transitions for Cu-BTTri Column Reactions with Glutathione Derivatives by TGA after Rinsing Treatment.

MOF (Substrate)[e]	T_o[a,b,c] (°C)	Weight Change[b,c,d] (Δ wt. %)
Cu-BTTri (H_2O)	144 (± 3)	1.1 (± 0.1)
Cu-BTTri (GSH)	173 (± 1)	1.8 (± 0.2)
Cu-BTTri (GSSG)	176 (± 2)	1.9 (± 0.2)
Cu-BTTri (GSNO)	167 (± 1)	2.1 (± 0.1)

[a] T_o calculated using TRIOS software; ΔT of 101 – 220 °C.
[b] Data reported as mean ± SD of $n = 3$ replicate measurements.
[c] Ramp 5 °C min^{-1} to 25 °C; isothermal @ 25 °C for 30 min; ramp 5 °C min^{-1} to 100 °C; isothermal @ 100 °C for 10 min; ramp 5 °C min^{-1} to 225 °C; isothermal @ 225 °C for 10 min.
[d] ΔT of 101 – 220 °C.
[e] 30 mg MOF Cu-BTTri loaded into 1 mL empty fritted SPE tube; 20 mL of 1 mM GS(X) solution flowed through MOF bed; 10 x 10 mL dd-H_2O rinses of MOF bed; vacuum dried (~ 1 Torr)

Mass spectrometry was used to identify species present and assess transformations in these MOF column reactions. The referenced mass adduct data for glutathione derivatives is given in Table 4. Analyses of the GSH solutions stock and effluent solutions displayed strong signals at *m*/*z* 308, attributed to protonated GSH adduct $[GSH + H]^+$ in these solutions. However, the rinsing solutions do not contain this peak at *m*/*z* 308. Instead, *m*/*z* peaks at 307 and 613 are observed,

consistent with the doubly and singly protonated GSSG adducts $[GSSG + 2H]^{2+}$ and $[GSSG + H]^{+}$ respectively, indicating the presence of GSSG in decreasing intensity in the rinse solutions. The tenth rinse shows these signals at <5 % of the intensity of the *m*/*z* 308 signal detected in the effluent. Mass spectral data for GSH column reaction solutions is shown in Figures SI 14-25. Analyses of the GSSG stock, effluent, and rinsing solutions are as anticipated. Peaks at *m*/*z* 307 and 613 are observed in decreasing intensity for all solutions, consistent with the presence of GSSG. The tenth rinse shows these signals at <5 % of the intensity of the signals for the effluent. Mass spectral data for GSSG column reaction solutions is shown in Figures SI 26-37. These data support that, under aerobic exposure to Cu-BTTri, GSH is oxidized to GSSG (although not upon the initial pass of the effluent through the column bed), which then strongly binds to Cu-BTTri. The uniformity in the thermal decomposition data for these two analytes is understandable as GSSG adsorbs to the Cu-BTTri framework in both cases.

Table 4. Mass Spectrometry Analytes for Glutathione Derivatives

Mass Spectrometry Adduct	Mass-to-Charge Ratio (*m*/*z*)
$[GS\cdot + H]^{+}$	307
$[GSSG + 2H]^{2+}$	307
$[GSH + H]^{+}$	308
$[GSNO + H]^{+}$	337
$[GSSG + H]^{+}$	613

Mass spectral analyses of the GSNO stock, effluent, and rinse solutions displayed strong signals at *m*/*z* 307 and *m*/*z* 337. These signals are attributed to the protonated GSNO adduct $[GSNO + H]^{+}$ and the protonated radical GS· adduct $[GS\cdot + H]^{+}$, confirming the presence of GSNO in decreasing intensity in all solutions. The tenth rinse shows these signals at <5 % of the intensity of the signals for the effluent. Mass spectral data for GSNO column reaction solutions is shown in Figures SI 38-49. The presence of the radical GS· species is likely due to homolytic cleave of the GS-NO bond under the conditions of the mass spectrometry method. Furthermore, this *m*/*z* 307 signal does not suggest the presence of GSSG via the doubly charged $[GSSG + 2H]^{2+}$ adduct as no accompanying *m*/*z* 613 signal for the singly charged $[GSSG + H]^{+}$ adduct is observed in any of the rinse solutions. This finding is intriguing since GSNO in aqueous media is known to oxidize to form GSSG when exposed to Cu-BTTri.[30] The aerobic conditions of the column reactions in this work may influence the ability of Cu-BTTri to catalyze the homolytic cleavage of the GS-NO bond, leading to unreacted GSNO bound to the MOF.[37] These MS studies corroborate the TGA studies showing that Cu-BTTri exposed to GSNO exhibits different thermal decomposition phenomena than Cu-BTTri exposed to GSH or GSSG.

III. Thermal Transitions and Associated Mass Spectra for Anaerobic Cu-BTTri Reactions with Glutathione Derivatives

Anaerobic reactions were prepared to investigate whether GSH, GSSG, and GSNO exposure to Cu-BTTri in aqueous reaction media would result in GS-X reaction products strongly binding to the MOF, producing distinct thermal decomposition profiles by TGA. The procedure for studying this reaction system is given below in Scheme 2. Binding of GS-X species to Cu-BTTri has important implications for the efficacy of Cu-BTTri in therapeutic applications as such binding may decrease or inhibit the MOF's ability to catalyze the oxidation of GSNO. The goal of these experiments was to determine if GS-X species would strongly bind to Cu-BTTri and if bound species could be distinguished from one another by means of thermal decomposition data as well as accompanying mass spectral analyses. The reaction supernatants were isolated both anaerobically via cannula transfer and aerobically via decantation for MS analyses to determine if any reactant transformations were due to exposure to aerobic conditions. Post reaction, the MOF powders were transferred to 1 mL empty fritted, SPE tubes to mimic the rinsing process of the Cu-BTTri column reactions.

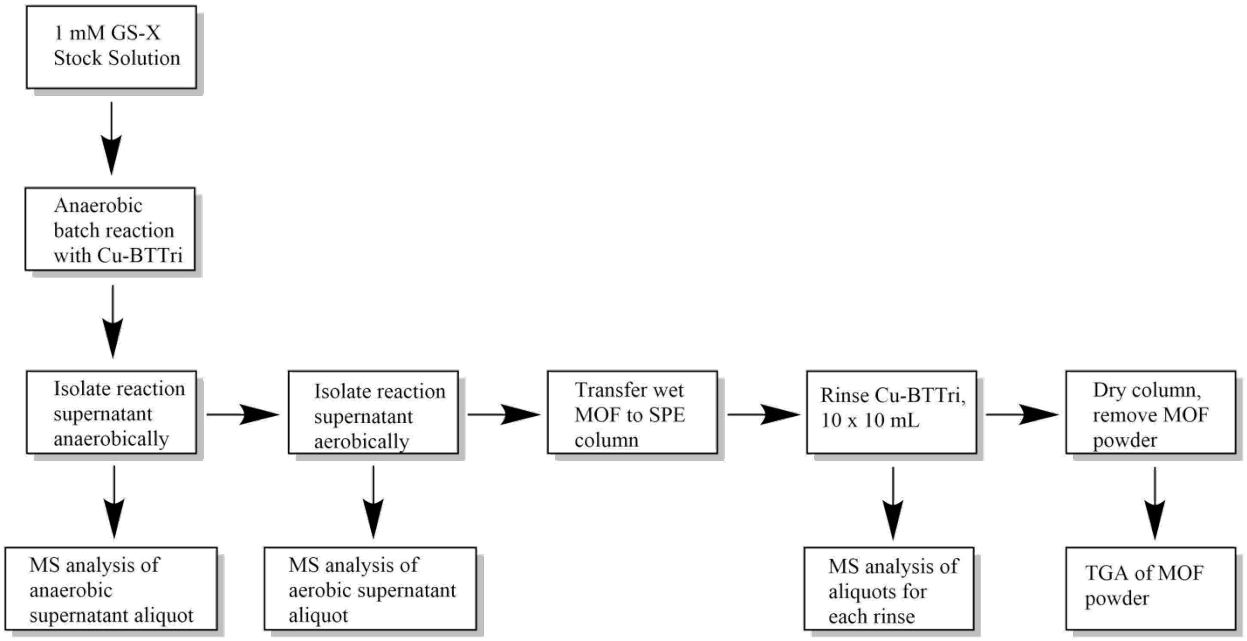

Scheme 2. Flowchart for the procedure and analysis of the aerobic Cu-BTTri column reactions with glutathione derivatives.

Table 5 gives the thermal onset temperatures and associated wt. % changes for the anaerobic Cu-BTTri reactions with 1 mM GSH, 1 mM GSSG, and 1 mM GSNO determined by TGA methods. All three reactions exhibited significantly different thermal onset temperatures from that

of Cu-BTTri alone (Table 3; $p < 0.001$), suggesting adsorption of GS-X species to the MOF. For Cu-BTTri reactions with GSH, GSSG, and GSNO, the thermal onset temperatures were determined at 184 (± 1) °C, 188 (± 1) °C, and 185 (± 1) °C, respectively. These onset temperatures were found to be statistically different from one another ($p < 0.001$) despite the relatively tight temperature range, 4 °C, of their observed decomposition phenomena.[38] Weight percent changes for Cu-BTTri exposed to GSH, GSSG, and GSNO were found to be 3.7 (± 0.2) %, 2.3 (± 0.3) %, and 2.2 (± 0.4) %, respectively. All 3 systems, much like the aerobic Cu-BTTri column reaction systems, display a mass loss greater than the dehydration of Cu-BTTri alone, indicating a substantial degree of chemisorption of GS-X analytes to the MOF.

Table 5. Thermal Transition Data for Cu-BTTri Anaerobic Reactions with Glutathione Derivatives by TGA after Rinsing Treatment.

Substrate[e]	T_o[a,b,c] (°C)	Weight Change[b,c,d] (Δ wt. %)
Cu-BTTri (GSH)	184 (± 1)	3.7 (± 0.2)
Cu-BTTri (GSSG)	188 (± 1)	2.3 (± 0.3)
Cu-BTTri (GSNO)	185 (± 1)	2.2 (± 0.4)

[a] T_o calculated using TRIOS software; ΔT of 101 – 220 °C.
[b] Data reported as mean ± SD of $n = 3$ replicate measurements.
[c] Ramp 5 °C min^{-1} to 25 °C; isothermal @ 25 °C for 30 min; ramp 5 °C min^{-1} to 100 °C; isothermal @ 100 °C for 10 min; ramp 5 °C min^{-1} to 225 °C; isothermal @ 225 °C for 10 min.
[d] ΔT of 101 – 220 °C.
[e] Anaerobic reaction preparation, including all sample preps and transfers; 50 mg MOF Cu-BTTri; 35 mL of 1 mM GS(X) solution; N_2 bubbling for 72 h @ RT; Supernatant isolated, Cu-BTTri solid transferred to 1 mL empty fritted SPE tubes; 10 x 10 mL dd-H_2O rinses of MOF bed; vacuum dried (~ 1 Torr)

Mass spectral analyses of all 3 Cu-BTTri (GS-X) systems gave similar results. For all 3 systems, the analyte signals observed were peaks at *m*/*z* 307 and 613, consistent with the doubly and singly protonated GSSG adducts $[GSSG + 2H]^{2+}$ and $[GSSG + H]^{+}$ respectively. By the 10th rinse, each system displayed signals <5 % of the intensity of the signals detected in the reaction supernatants. Mass spectral data for the anaerobic batch reaction solutions is shown in Figures SI 50-85. All 3 studies showed no variation in signal intensity between the anaerobic and aerobic reaction supernatants, suggesting that any chemical transformations due to anaerobic Cu-BTTri exposure occurred during the reaction and not because of the post-reaction aerobic workup protocols. These findings, considered together with the absence of peaks at *m*/*z* 308 and 337 attributed to the presence of GSH and GSNO adducts, suggest that chemisorption of GSSG to Cu-BTTri is the primary phenomena observed in all 3 systems. While this result is unsurprising for the GSSG control reaction, the oxidation of both GSH and GSNO occurred despite exclusion of dioxygen from the reactions. Thus, the oxidations appear to be promoted by the exposure of GSH

and GSNO to Cu-BTTri. These studies clearly indicate that the catalytic oxidation of GSNO by Cu-BTTri does not occur without potentially deleterious binding of reaction by-products to the MOF, which could lead to decreased catalytic efficacy. Furthermore, such binding of reaction by-products is not limited to this reaction alone as similar findings were observed for the free thiol GSH. While the anaerobic oxidation of GSNO to GSSG by Cu-BTTri has been reported, the analogous anaerobic oxidation of GSH to GSSG by Cu-BTTri is a new finding.[30] This discovery is a subject of ongoing investigation by the authors.

Conclusions

This work demonstrates the utility of TGA as a simple and rapid technique to examine chemisorption of analytes to metal–organic frameworks by distinguishing between reactants, products, and potential by-products of a reaction. Thermal methods were established to examine the byproducts irreversibly chemisorbed on Cu-BTTri post catalytic oxidation of GSNO. This behavior was validated by further experiments with adsorption of aqueous GSSG to Cu-BTTri and the catalytic oxidation of GSH by Cu-BTTri. These studies revealed that GSSG exhibited strong chemisorption to the MOF. Thermal analyses may lead to rapid validation of recycling protocols for Cu-BTTri, such as Soxhlet extraction or extensive washing with dd-H_2O. Similar thermal studies could be used to elucidate other important information with regards to MOF reactivity, such as reduced catalytic efficiency from poisoning, recyclability, and loading capacities of contaminants or toxins. Moreover, thermal methods accompanied by mass spectrometry can provide substantial detail about the nature of chemical transformations facilitated by the MOF and weakly versus irreversibly adsorbed chemical species. The use of TGA-MS instrumentation to acquire mass adduct or fragmentation data while simultaneously examining thermal transitions allows for direct identification of chemisorbed analytes during decomposition or desorption from the MOF as well as potential development of quantitative thermal analysis methods. An additional consideration is whether Brunauer-Emmett-Teller (BET) surface area analysis could be employed along with TGA methods to determine if MOF chemisorption was primarily occurring on the surface or within the interior of the framework.

Acknowledgments

The authors would like to thank Jonathan E. Thai for synthesis of 1,3,5-tris(1*H*-1,2,3-triazol-5-yl)benzene and metal organic framework $H_3[(Cu_4Cl)_3(BTTri)_8]$. The authors would also like to thank Yanyi Zhang for synthesis of *S*-nitrosoglutathione.

Corresponding Author

* E-mail: melissa.reynolds@colostate.edu; Tel: + 1 970 491 3775.

Disclosure Statement
The authors declare no conflicts of interest.

Funding
W.M.J. was supported by the National Institutes of Health (5R21EB016838). J.B.T. was supported by the National Institutes of Health (5R01HL140301).

References

1. Zhao, X.; Wang, Y. X.; Li, D. S.; Bu, X. H.; Feng, P. Y., Metal-Organic Frameworks for Separation. *Adv. Mater.* **2018,** *30* (37).
2. Yuan, S.; Feng, L.; Wang, K. C.; Pang, J. D.; Bosch, M.; Lollar, C.; Sun, Y. J.; Qin, J. S.; Yang, X. Y.; Zhang, P.; Wang, Q.; Zou, L. F.; Zhang, Y. M.; Zhang, L. L.; Fang, Y.; Li, J. L.; Zhou, H. C., Stable Metal-Organic Frameworks: Design, Synthesis, and Applications. *Adv. Mater.* **2018,** *30* (37).
3. Yang, D.; Gates, B. C., Catalysis by Metal Organic Frameworks: Perspective and Suggestions for Future Research. *ACS Catal.* **2019,** *9* (3), 1779-1798.
4. Xu, Y. X.; Li, Q.; Xue, H. G.; Pang, H., Metal-organic frameworks for direct electrochemical applications. *Coord. Chem. Rev.* **2018,** *376*, 292-318.
5. Xu, C. P.; Fang, R. Q.; Luque, R.; Chen, L. Y.; Li, Y. W., Functional metal-organic frameworks for catalytic applications. *Coord. Chem. Rev.* **2019,** *388*, 268-292.
6. Woellner, M.; Hausdorf, S.; Klein, N.; Mueller, P.; Smith, M. W.; Kaskel, S., Adsorption and Detection of Hazardous Trace Gases by Metal-Organic Frameworks. *Adv. Mater.* **2018,** *30* (37).
7. Wang, H.; Lustig, W. P.; Li, J., Sensing and capture of toxic and hazardous gases and vapors by metal-organic frameworks. *Chem. Soc. Rev.* **2018,** *47* (13), 4729-4756.
8. Jiao, L.; Wang, Y.; Jiang, H. L.; Xu, Q., Metal-Organic Frameworks as Platforms for Catalytic Applications. *Adv. Mater.* **2018,** *30* (37).
9. Jiao, L.; Seow, J. Y. R.; Skinner, W. S.; Wang, Z. U.; Jiang, H. L., Metal-organic frameworks: Structures and functional applications. *Mater. Today* **2019,** *27*, 43-68.
10. Feng, M. B.; Zhang, P.; Zhou, H. C.; Sharma, V. K., Water-stable metal-organic frameworks for aqueous removal of heavy metals and radionuclides: A review. *Chemosphere* **2018,** *209*, 783-800.
11. Dhakshinamoorthy, A.; Li, Z. H.; Garcia, H., Catalysis and photocatalysis by metal organic frameworks. *Chem. Soc. Rev.* **2018,** *47* (22), 8134-8172.
12. Chedid, G.; Yassin, A., Recent Trends in Covalent and Metal Organic Frameworks for Biomedical Applications. *Nanomaterials* **2018,** *8* (11).
13. Bobbitt, N. S.; Mendonca, M. L.; Howarth, A. J.; Islamoglu, T.; Hupp, J. T.; Farha, O. K.; Snurr, R. Q., Metal-organic frameworks for the removal of toxic industrial chemicals and chemical warfare agents. *Chem. Soc. Rev.* **2017,** *46* (11), 3357-3385.
14. Barea, E.; Montoro, C.; Navarro, J. A. R., Toxic gas removal - metal-organic frameworks for the capture and degradation of toxic gases and vapours. *Chem. Soc. Rev.* **2014,** *43* (16), 5419-5430.
15. Hartmann, M.; Kunz, S.; Himsl, D.; Tangermann, O.; Ernst, S.; Wagener, A., Adsorptive separation of isobutene and isobutane on Cu(3)(BTC)(2). *Langmuir* **2008,** *24* (16), 8634-8642.

16. Ploskonka, A. M.; DeCoste, J. B., Tailoring the Adsorption and Reaction Chemistry of the Metal -Organic Frameworks UiO-66, UiO-66-NH2, and HKUST-1 via the Incorporation of Molecular Guests. *ACS Appl. Mater. Interfaces* **2017,** *9* (25), 21579-21585.
17. Cai, J. M.; Xu, D.; Dong, Z. J.; Yu, X.; Yang, Y.; Banks, S. W.; Bridgwater, A. V., Processing thermogravimetric analysis data for isoconversional kinetic analysis of lignocellulosic biomass pyrolysis: Case study of corn stalk. *Renew. Sust. Energ. Rev.* **2018,** *82*, 2705-2715.
18. Mohamedali, M.; Henni, A.; Ibrahim, H., Markedly improved CO2 uptake using imidazolium-based ionic liquids confined into HKUST-1 frameworks. *Microporous Mesoporous Mater.* **2019,** *284*, 98-110.
19. Bae, Y. S.; Dubbeldam, D.; Nelson, A.; Walton, K. S.; Hupp, J. T.; Snurr, R. Q., Strategies for Characterization of Large-Pore Metal-Organic Frameworks by Combined Experimental and Computational Methods. *Chem. Mater.* **2009,** *21* (20), 4768-4777.
20. Matsuyama, K.; Hayashi, N.; Yokomizo, M.; Kato, T.; Ohara, K.; Okuyama, T., Supercritical carbon dioxide-assisted drug loading and release from biocompatible porous metal-organic frameworks. *J. Mater. Chem. B* **2014,** *2* (43), 7551-7558.
21. Lan, X. Y.; Zhang, H. H.; Bai, P.; Guo, X. H., Investigation of metal organic frameworks for the adsorptive removal of hydrochloride from dilute aqueous solution. *Microporous Mesoporous Mater.* **2016,** *231*, 40-46.
22. Bodkhe, G. A.; Deshmukh, M. A.; Patil, H. K.; Shirsat, S. M.; Srihari, V.; Pandey, K. K.; Panchal, G.; Phase, D. M.; Mulchandani, A.; Shirsat, M. D., Field effect transistor based on proton conductive metal organic framework (CuBTC). *J. Phys. D.: Appl. Phys.* **2019,** *52* (33).
23. Zhang, W. H.; Kauer, M.; Guo, P. H.; Kunze, S.; Cwik, S.; Muhler, M.; Wang, Y. M.; Epp, K.; Kieslich, G.; Fischer, R. A., Impact of Synthesis Parameters on the Formation of Defects in HKUST-1. *Eur. J. Inorg. Chem.* **2017,** (5), 925-931.
24. Li, N.; Mu, B.; Lv, L.; Huang, R. D., Assembly of new polyoxometalate-templated metal-organic frameworks based on flexible ligands. *J. Solid State Chem.* **2015,** *226*, 88-93.
25. Liu, B.; Yang, J.; Yang, G. C.; Ma, J. F., Four New Three-Dimensional Polyoxometalate-Based Metal-Organic Frameworks Constructed From Mo6O18(O3AsPh)(2) (4-) Polyoxoanions and Copper(I)-Organic Fragments: Syntheses, Structures, Electrochemistry, and Photocatalysis Properties. *Inorg. Chem.* **2013,** *52* (1), 84-94.
26. Petit, C.; Mendoza, B.; Bandosz, T. J., Hydrogen Sulfide Adsorption on MOFs and MOF/Graphite Oxide Composites. *ChemPhysChem* **2010,** *11* (17), 3678-3684.
27. Lan, Y. Q.; Li, S. L.; Wang, X. L.; Shao, K. Z.; Du, D. Y.; Zang, H. Y.; Su, Z. M., Self-assembly of polyoxometalate-based metal organic frameworks based on octamolybdates and copper-organic units: from Cu-II, Cu-I,Cu-II to Cu-I via changing organic amine. *Inorg. Chem.* **2008,** *47* (18), 8179-8187.
28. Cheng, Y.; Kondo, A.; Noguchi, H.; Kajiro, H.; Urita, K.; Ohba, T.; Kaneko, K.; Kanoh, H., Reversible Structural Change of Cu-MOF on Exposure to Water and Its CO2 Adsorptivity. *Langmuir* **2009,** *25* (8), 4510-4513.
29. Demessence, A.; D'Alessandro, D. M.; Foo, M. L.; Long, J. R., Strong CO2 Binding in a Water-Stable, Triazolate-Bridged Metal-Organic Framework Functionalized with Ethylenediamine. *J. Am. Chem. Soc.* **2009,** *131* (25), 8784-+.
30. Tuttle, R. R.; Rubin, H. N.; Rithner, C. D.; Finke, R. G.; Reynolds, M. M., Copper ion vs copper metal-organic framework catalyzed NO release from bioavailable S-Nitrosoglutathione en route to biomedical applications: Direct 1H NMR monitoring in water allowing identification of

the distinct, true reaction stoichiometries and thiol dependencies. *J. Inorg. Biochem.* **2019,** *199*, 110760.
31. Neufeld, M. J.; Lutzke, A.; Jones, W. M.; Reynolds, M. M., Nitric Oxide Generation from Endogenous Substrates Using Metal-Organic Frameworks: Inclusion within Poly(vinyl alcohol) Membranes To Investigate Reactivity and Therapeutic Potential. *ACS Appl. Mater. Interfaces* **2017,** *9* (41), 35628-35641.
32. Neufeld, M. J.; Lutzke, A.; Tapia, J. B.; Reynolds, M. M., Metal-Organic Framework/Chitosan Hybrid Materials Promote Nitric Oxide Release from S-Nitrosoglutathione in Aqueous Solution. *ACS Appl. Mater. Interfaces* **2017,** *9* (6), 5139-5148.
33. Hart, T. W., Some observations concerning the S-nitroso and S-phenylsulphonyl derivatives of L-cysteine and glutathione. *Tetrahedron Lett.* **1985,** *26* (16), 2013-2016.
34. Parent, M.; Dahboul, F.; Schneider, R.; Clarot, I.; Maincent, P.; Leroy, P.; Boudier, A., A Complete Physicochemical Identity Card of *S*-nitrosoglutathione. *Curr. Pharm. Anal.* **2013,** *9* (1), 31-42.
35. Haynes, W. M., *CRC Handbook of Chemistry and Physics*. 92nd ed.; CRC Press: Boca Raton, FL, 2011.
36. Melvin, A. C.; Jones, W. M.; Lutzke, A.; Allison, C. L.; Reynolds, M. M., S-Nitrosoglutathione exhibits greater stability than S-nitroso-N-acetylpenicillamine under common laboratory conditions: A comparative stability study. *Nitric Oxide* **2019,** *92*, 18-25.
37. Dicks, A. P.; Swift, H. R.; Williams, D. L. H.; Butler, A. R.; AlSadoni, H. H.; Cox, B. G., Identification of Cu+ as the effective reagent in nitric oxide formation from *S*-nitrosothiols (RSNO). *J. Chem. Soc.-Perkin Trans. 2* **1996,** (4), 481-487.
38. E2550-17 Standard Test Method for Thermal Stability by Thermogravimetry. ASTM International: West Conshohocken, PA, 2017.

*******Additional copies of tables, figures, and schemes are included below this line for formatting and organizational purposes as necessary by those at *Langmuir*. These figures are already in-line where they belong in the text and do not represent additional, original content for the article after the references listed above on pgs. 16-18. ***** - W.M. Jones**

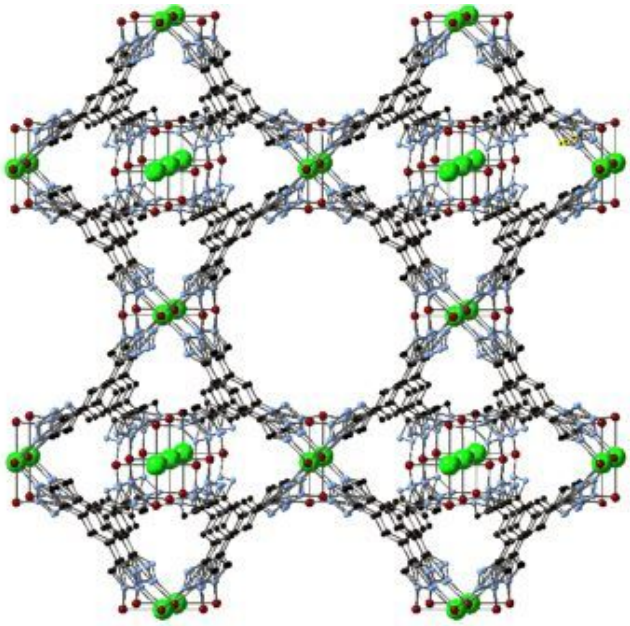

Figure 1. Structure of MOF Cu-BTTri, $H_3[(Cu_4Cl)_3(BTTri)_8]$. Carbon atoms depicted in black; chlorine atoms depicted in green; copper atoms depicted in red; hydrogen atoms omitted for clarity; nitrogen atoms depicted in blue.

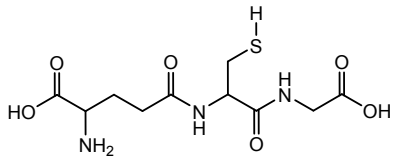

Glutathione (GSH)

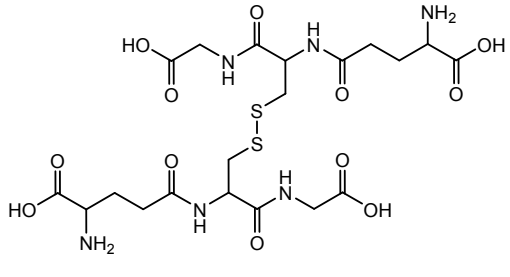

Glutathione disulfide (GSSG)

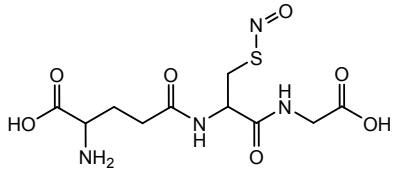

S-nitrosoglutathione (GSNO)

Figure 2. Structures of glutathione (GSH), glutathione disulfide (GSSG) and *S*-nitrosoglutathione (GSNO).

Table 1. Thermal Transitions of Glutathione Derivatives Measured by TGA

Substrate	Onset Temperature (T_o - °C)[a,b,c]	
GSH	192 (± 1)	-
GSSG	179 (± 1)	-
GSNO	143 (± 1)	189 (± 1)

[a] T_o calculated using TRIOS software; ΔT of 101-220 °C for GSH/GSSG; ΔT_1 of 101-155 °C, ΔT_2 of 155 – 220 °C for GSNO.
[b] Data reported as mean ± SD of n = 3 replicate measurements.
[c] Ramp 5 °C min^{-1} to 25 °C; isothermal @ 25 °C for 30 min; ramp 5 °C min^{-1} to 100 °C; isothermal @ 100 °C for 10 min; ramp 5 °C min^{-1} to 225 °C; isothermal @ 225 °C for 10 min.

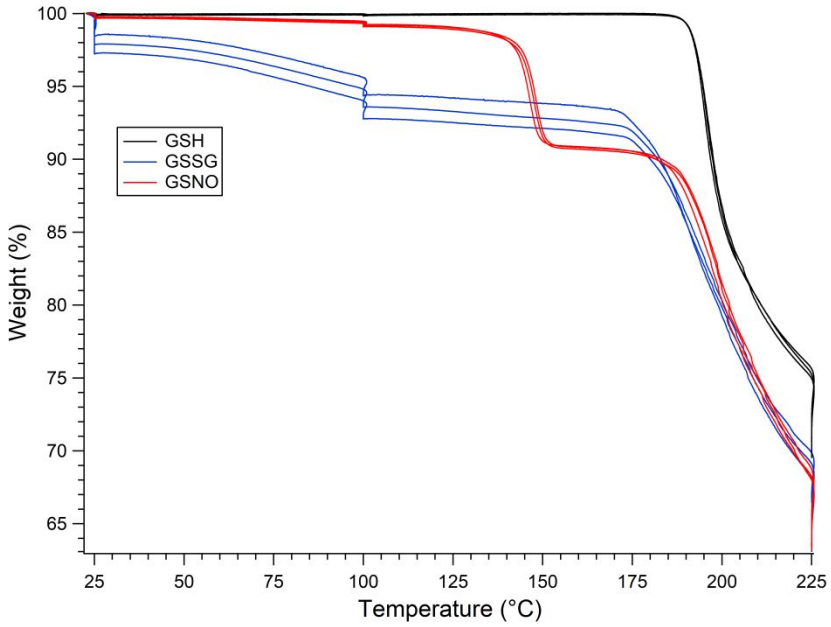

Figure 3. Resolution of the thermal decomposition phenomena of GSH (black), GSSG (blue), and GSNO (red) by TGA. Replicate measurements (n = 3) are shown for each sample.

Table 2. Weight Change of Cu-BTTri from Ambient Conditions by TGA

Cu-BTTri Weight Change from Ambient Conditions[a,b,c]	
ΔT	Δ wt. %
25 – 101 °C	12 (± 8)
101 – 220 °C	1.1 (± 0.1)

[a] Data reported as mean ± SD of n = 3 replicate measurements.

[b] Ramp 5 °C min^{-1} to 25 °C; isothermal @ 25 °C for 30 min; ramp 5 °C min^{-1} to 100 °C; isothermal @ 100 °C for 10 min; ramp 5 °C min^{-1} to 225 °C; isothermal @ 225 °C for 10 min.
[c] 30 mg MOF Cu-BTTri loaded into 1 mL empty fritted SPE tube; 20 mL of dd-H_2O flowed through MOF bed; vacuum dried (~ 1 Torr)

Table 3. Thermal Transitions for Cu-BTTri Column Reactions with Glutathione Derivatives by TGA after Rinsing Treatment.

MOF (Substrate)[e]	T_o[a,b,c] (°C)	Weight Change[b,c,d] (Δ wt. %)
Cu-BTTri (H_2O)	144 (± 3)	1.1 (± 0.1)
Cu-BTTri (GSH)	173 (± 1)	1.8 (± 0.2)
Cu-BTTri (GSSG)	176 (± 2)	1.9 (± 0.2)
Cu-BTTri (GSNO)	167 (± 1)	2.1 (± 0.1)

[a] T_o calculated using TRIOS software; ΔT of 101 – 220 °C.
[b] Data reported as mean ± SD of $n = 3$ replicate measurements.
[c] Ramp 5 °C min^{-1} to 25 °C; isothermal @ 25 °C for 30 min; ramp 5 °C min^{-1} to 100 °C; isothermal @ 100 °C for 10 min; ramp 5 °C min^{-1} to 225 °C; isothermal @ 225 °C for 10 min.
[d] ΔT of 101 – 220 °C.
[e] 30 mg MOF Cu-BTTri loaded into 1 mL empty fritted SPE tube; 20 mL of 1 mM GS(X) solution flowed through MOF bed; 10 x 10 mL dd-H_2O rinses of MOF bed; vacuum dried (~ 1 Torr)

Table 4. Mass Spectrometry Analytes for Glutathione Derivatives

Mass Spectrometry Adduct	Mass-to-Charge Ratio (m/z)
$[GS\cdot + H]^+$	307
$[GSSG + 2H]^{2+}$	307
$[GSH + H]^+$	308
$[GSNO + H]^+$	337
$[GSSG + H]^+$	613

Table 5. Thermal Transition Data for Cu-BTTri Anaerobic Reactions with Glutathione Derivatives by TGA after Rinsing Treatment.

Substrate[e]	T_o[a,b,c] (°C)	Weight Change[b,c,d] (Δ wt. %)
Cu-BTTri (GSH)	184 (± 1)	3.7 (± 0.2)
Cu-BTTri (GSSG)	188 (± 1)	2.3 (± 0.3)
Cu-BTTri (GSNO)	185 (± 1)	2.2 (± 0.4)

[a] T_o calculated using TRIOS software; ΔT of 101 – 220 °C.
[b] Data reported as mean ± SD of $n = 3$ replicate measurements.
[c] Ramp 5 °C min^{-1} to 25 °C; isothermal @ 25 °C for 30 min; ramp 5 °C min^{-1} to 100 °C; isothermal @ 100 °C for 10 min; ramp 5 °C min^{-1} to 225 °C; isothermal @ 225 °C for 10 min.
[d] ΔT of 101 – 220 °C.

[e] Anaerobic reaction preparation, including all sample preps and transfers; 50 mg MOF Cu-BTTri; 35 mL of 1 mM GS(X) solution; N_2 bubbling for 72 h @ RT; Supernatant isolated, Cu-BTTri solid transferred to 1 mL empty fritted SPE tubes; 10 x 10 mL dd-H_2O rinses of MOF bed; vacuum dried (~ 1 Torr)

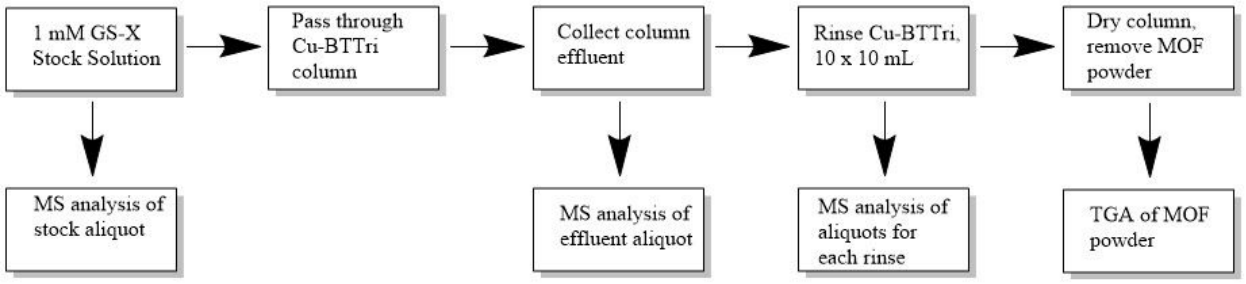

Scheme 1. Flowchart for the procedure and analysis of the aerobic Cu-BTTri column reactions with glutathione derivatives.

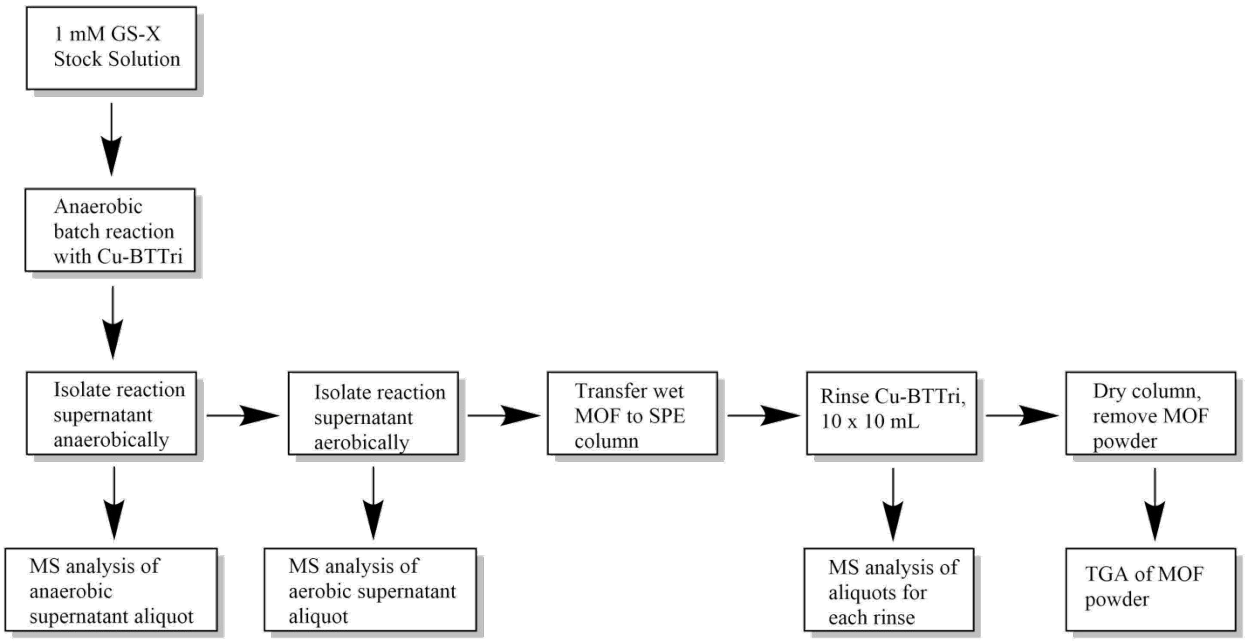

Scheme 2. Flowchart for the procedure and analysis of the aerobic Cu-BTTri column reactions with glutathione derivatives.

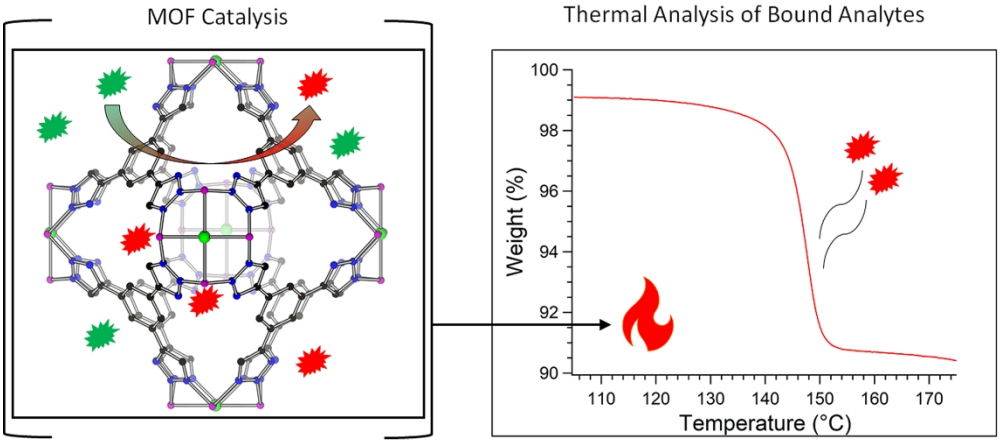

338x190mm (300 x 300 DPI)